J. Phys. D: Appl. Phys. 40 (2007) 3985–3990 doi:10.1088/0022-3727/40/13/011

Cross-sectional transmission electron microscopy observations on the Berkovich indentation-induced deformation microstructures in GaN thin films

Chi-Hui Chien[1], Sheng-Rui Jian[2,6], Chung-Ting Wang[1], Jenh-Yih Juang[2,3], J C Huang[4] and Yi-Shao Lai[5]

[1] Department of Mechanical and Electro-Mechanical Engineering; Center for Nanoscience and Nanotechnology, National Sun Yat-sen University, Kaohsiung 804, Taiwan
[2] Department of Electrophysics, National Chiao Tung University, Hsinchu 300, Taiwan
[3] Department of Physics, National Taiwan Normal University, Taipei 106, Taiwan
[4] Institute of Materials Science and Engineering; Center for Nanoscience and Nanotechnology, National Sun Yat-Sen University, Kaohsiung 804, Taiwan
[5] Central Labs, Advanced Semiconductor Engineering, Inc. 26 Chin 3rd Rd., Nantze Export Processing Zone, 811 Nantze, Kaohsiung, Taiwan

E-mail: srjian@gmail.com

Received 8 February 2007, in final form 17 May 2007
Published 15 June 2007
Online at stacks.iop.org/JPhysD/40/3985

Abstract
Nanoindentation-induced mechanical deformation in GaN thin films prepared by metal-organic chemical-vapour deposition was investigated using the Berkovich diamond tip in combination with the cross-sectional transmission electron microscopy (XTEM). By using focused ion beam milling to accurately position the cross-section of the indented region, the XTEM results demonstrate that the major plastic deformation was taking place through the propagation of dislocations. The present observations are in support of attributing the pop-ins that appeared in the load–displacement curves to the massive dislocation activities occurring underneath the indenter during the loading cycle. The absence of indentation-induced new phases might have been due to the stress relaxation via the substrate and is also consistent with the fact that no discontinuity was found upon unloading.

(Some figures in this article are in colour only in the electronic version)

1. Introduction

The development of microsystems and nanotechnology has relied, in many ways, on the major progress accomplished in surface science and materials science and, in particular, thin film technology. In the past, much effort has been devoted to characterizing the optical, electrical and magnetic properties of the resultant structures and devices. Recently, it has become clear that, in order to fully harvest the unprecedented potential of the emerging nanotechnologies in general, the processes-induced structural and mechanical modifications on the materials might be equally important. For instance, over the last two decades, gallium nitride (GaN) epitaxial films and devices have attracted considerable attention because of their broad applications in blue/green light emitting diodes [1], laser diodes and photodetectors [2], as well as high-power or high-temperature electronics [3]. However, the successful fabrication of devices based on epitaxial GaN thin films requires a better understanding of the mechanical characteristics in addition to their optical and electrical

[6] Author to whom any correspondence should be addressed.

performance, since the contact loading during processing or packaging can significantly degrade the performance of these devices. Consequently, there is a growing demand for investigating the mechanical characteristics of materials, in particular in the nanoscale regime, for device applications.

In trying to mimic the contact loading frequently encountered in wire-bonding packaging, there are several issues to be addressed. Firstly, the mechanical responses of a thin film to an applied load might be vastly different from that of the same bulk material. For this purpose, unfortunately, the traditional methods such as tensile measurements do not scale well into the micrometre and nanometre scale. Secondly, the role of structural changes under contact loading are largely underestimated owing to the difficulties in probing the structural characterizations of thin films affected by the contact interaction directly. In this respect, the advent of nanoindentation instruments and the subsequent development of the underlying science may potentially address the scaling issue and the scientific evaluation of all contact loading related phenomena. Since the deformation that occurred during the test is controlled locally on the nanometre scale, nanoindentation has, recently, been widely used to investigate the deformation mechanisms of various semiconductors [4–6], in combination with the molecular dynamics simulations for analysing the atomic interactions [7–9]. In addition, the mechanical properties of surfaces of solids and thin films, such as the hardness and Young's modulus, have been extracted using this technique [10–12].

Despite the successes obtained from the nanoindentation studies in GaN thin films, this technique itself does not provide direct information on subsurface deformation mechanisms, crack initiation and dislocation propagation. Therefore, complementary methods capable of providing such information are needed. In most nanoindentation studies, both Raman microspectroscopy [5] and plan-view TEM [6] techniques have been successfully used to analyse the phase transformation and defect/dislocations propagation along the horizontal direction of materials. However, they are inadequate to distinguish the phase changes inside the deformed zone along the direction of the concentrated applied stress. The focused ion beam (FIB) miller, which is now widely used for a range of material characterization applications [4], is an excellent tool for preparing transmission electron microscopy samples to reveal the cross-sectional microstructure of the locally deformed regions. In this report, we employed this method to investigate the subsurface deformation structures as well as the possible substrate deformations involved in the Berkovich nanoindentation performed on GaN films. The detailed microstructure evolution resulting from the perpendicularly contact-induced deformed region was examined to correlate with the features exhibited in the obtained load–displacement measurements.

2. Experimental details

The GaN thin films used in this study were grown on (0 0 0 1)-sapphire substrates by the metal-organic chemical-vapour deposition (MOCVD) method with an average thickness of about 2 μm. The detailed growth procedures of the GaN thin films can be found elsewhere [13]. The nanoindentation measurements were performed on a Nanoindenter MTS NanoXP® system (MTS Cooperation, Nano Instruments Innovation Center, TN, USA) with a diamond pyramid-shaped Berkovich-type indenter tip, whose radius of curvature is 50 nm. The mechanical properties (the hardness and Young's modulus) of GaN thin films were measured by nanoindentation with a continuous stiffness measurements (CSM) technique [14]. In this technique, a small sinusoidal load with known frequency and amplitude was superimposed onto the quasi-static load. It results in a modulation of the indenter displacement that is phase shifted in response to the excitation force. The stiffness, S, of the material, and the damping, wC, along indentation loading can be respectively calculated using equations (1) and (2) expressed below. The hardness and elastic modulus are, then, calculated by putting the obtained stiffness data into equations (3) and (4), respectively. In this way, the hardness and modulus as a function of penetration depth are determined for a single loading–unloading cycle [15].

$$S = \left[\frac{1}{(P_{\max}/h(w))\cos\Phi - (K_s - mw^2)} - K_f^{-1}\right]^{-1}, \qquad (1)$$

$$wC = \frac{P_0}{h(w)}\sin\Phi, \qquad (2)$$

$$H = \frac{P_{\max}}{A_c}, \qquad (3)$$

$$\frac{E}{1-v^2} = \frac{\sqrt{\pi}}{2}\frac{1}{\sqrt{A_c}}, \qquad (4)$$

where $P_{\max}$ and $h(w)$ are denoted as the driving force and the displacement response of the indenter, respectively; Φ is the phase angle between $P_{\max}$ and $h(w)$; m is the mass of the indenter column; K_s is the is spring constant in the vertical direction; K_f is frame stiffness; m, K_s and K_f are all constant values for the specified indentation system; w is angular speed which equals $2\pi f$; f is the driven frequency of the ac signal of 45 Hz for this work, which is used to avoid the sensitivity to thermal drift; the loading resolution of the system was 50 nN; v is Poisson's ratio and set to be 0.25 [13] for current analysis; and A_c is the contact area when the material in contact with indenter being loaded at $P_{\max}$.

The area function, which is used to calculate contact area, A_c, from contact depth, h_c, was carefully calibrated by using fused silica as the standard sample prior to the nanoindentation experiments. The nanoindentation tests were carried out in the following sequence: first of all, the Berkovich indenter was brought into contact with the surface at a constant strain rate of 0.05 s^{-1} until 100 nm of penetration was achieved. The load was then held at the maximum value for 30 s in order to determine the creep behaviour. The Berkovich indenter was then withdrawn from the surface at the same rate until 10% of the maximum load was reached. This constant strain rate was chosen such that the strain-hardening effect could be avoided during the measurements. At least 10 indents were performed on each GaN film. The nanoindentations were sufficiently spaced to prevent mutual interactions. The hardness and Young's modulus of GaN films obtained from the present nanoindentation tests with CSM technique are

Table 1. Mechanical properties of GaN thin films derived from various measurement methods.

	GaN thin films	*H* (GPa)	*E* (GPa)	Indenter tip
Drovy *et al* [16]	As-grown	12 ± 2	287	Vickers
Nowak *et al* [17]	As-grown	20	295	Spherical
Kucheyev *et al* [18]	As-Grown	13.4	233	Spherical
	Ion-damaged	15.1	164	
	Ion-damaged	15.1	164	
	Amorphized	2.4	65	
Jian *et al* [13]	As-grown	19.34 ± 2.13	314.93 ± 40.58	Berkovich
	Si-doped	20.12 ± 2.51	247.16 ± 14.89	
Kavouras *et al* [19]	As-grown	13.67 ± 0.15	—	Knoop
	O-doped	14.74 ± 0.22	—	
	Mg-doped	16.87 ± 0.13	—	
	Au-doped	12.16 ± 0.09	—	
	Xe-doped	11.35 ± 0.12	—	
	Ar-doped	9.98 ± 0.14	—	
Chien *et al* [a]	As-grown	19.31 ± 1.05	286.12 ± 25.34	Berkovich

[a] This study.

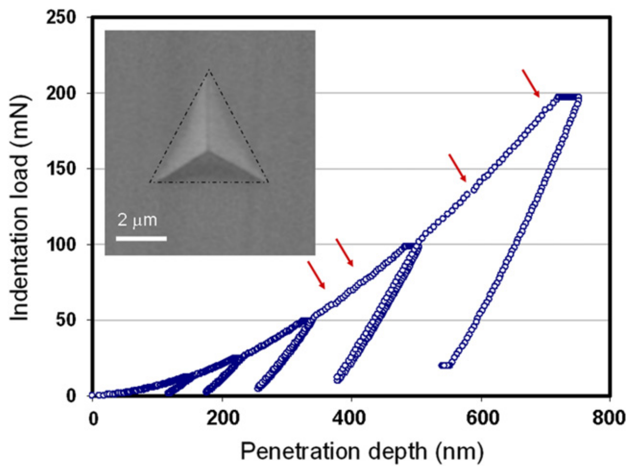

Figure 1. Typical cyclic nanoindentation load–displacement curves for GaN thin films obtained with a Berkovich indenter. The results show clear pop-in behaviours (indicated by the arrows) during loading, while no pop-out is evident in the unloading segments, indicating that no phase transition is involved. The inset is a SEM micrograph of an indent at an applied load of 200 mN. No apparent material pile-up around the indented area is evident.

19.31 ± 1.05 GPa and 286.12 ± 25.34 GPa, respectively. As displayed in table 1, which summarizes the hardness and Young's modulus for various GaN samples obtained from different indentation methods [16–19], the values obtained by using Berkovich indenter are somewhat larger than those obtained by other methods. Nonetheless, the current data are consistent with our previous studies [13], indicating the reproducibility of the technique.

Furthermore, in order to reveal the role played by the nucleation and propagation of dislocations in indentation-induced deformation, cyclic nanoindentation tests were also performed in this study. These tests were carried out by the following sequences. First, the indenter was loaded to some chosen load and then unloaded by 90% of the previous load, which completed the first cycle. It then was reloaded to a larger chosen load and unloaded by 90% for the second cycle. Figure 1 illustrated a typical cyclic indentation test repeated for 5 cycles. It is noted that in each cycle, the indenter was held for 30 s at 10% of its previous maximum load for thermal drift correction and for assuring that complete unloading was achieved. The thermal drift was kept below $\pm 0.05\,\mathrm{nm\,s^{-1}}$ for all indentations considered in this study. The same loading–unloading rate of $10\,\mathrm{mN\,s^{-1}}$ was used.

After indentation to a maximum load of 200 mN, the cross-sectional transmission electron microscopy (XTEM) samples of the GaN films were prepared by the lift-out technique using a dual-beam FIB station (FEI Nova 220). The technique for sample preparation using the FIB consisted of first milling two crosses alongside the indented area, serving as makers, and then depositing a layer of Pt (about 1 μm thick) to protect the area of interest from damages and implantation by the injected Ga^{+} ion beam. Material was removed from both sides of the selected area using an ion current of 5 nA, followed by successive thinning steps by reducing the ion current progressively from 3 nA to 300 pA until the foil was about 1 μm thick. Subsequently, the bottom and one side of the foil were cut free while tilting the sample at an angle of 45° to the ion beam. A central area containing the indentation apex of a few micrometres in length was then chosen and thinned further to a thickness of 100 nm, leaving the side thicker areas relatively intact to prevent the foil from collapsing. Finally a small area of interest was selected and thinned until electron transparency was achieved. The FIB milling procedures are displayed in figure 2. The transfer of the sample from the sample holder to the TEM grid with a carbon membrane was made *ex situ* using the electrostatic force of a glass needle. The TEM samples were examined in JEOL-2010F TEM operating at an accelerating voltage of 200 kV.

3. Results and discussion

As described above, figure 1 is a typical cyclic load–displacement plot for GaN thin film with a maximum load up to 200 mN. It is evident that for load below 50 mN, the load–displacement curve appears to be rather smooth during the whole loading–unloading cycle. However, it starts to exhibit irregularities, characterized by small sudden displacement

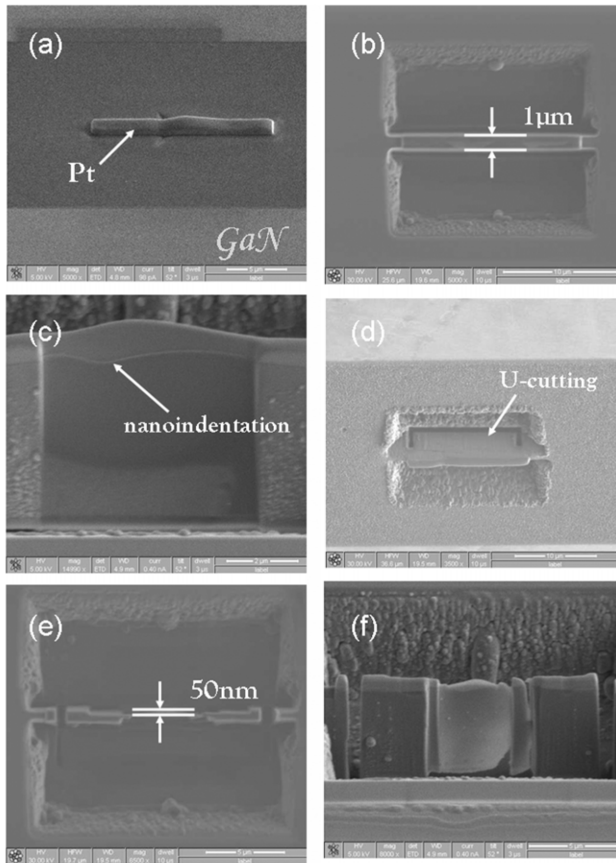

Figure 2. Illustration of the typical procedures for FIB milling sample preparation. Sample preparation starts with a line of nanoindentations. After depositing a protection layer of Pt (*a*), two big trenches are etched on either side of the indentation line (*b*) by a high current ion beam (7–20 nA). Further thinning of the middle strip involves a lower beam current ranging from 3 nA to 300 pA and leaves behind between the trenches a thin membrane around 300 nm thick (*c*). An ion dose of 50 pA is adopted for final cleaning steps and thinned further to a thickness of 100 nm. Then, cutting on the bottom (U-cutting) and both side edges releases the thin membrane (*d*)–(*e*). The sample (*f*) can be plucked by a shape glass tip under an optical microscopy outside the FIB station. Finally, the sample is delivered onto a carbon coated TEM grid.

excursions ('pop-ins') indicated by the arrows, during loading. The first apparent pop-in occurred at a load about 60 mN. Subsequently, the pop-ins phenomena are randomly distributed on the loading curve. We note here that the critical applied load for direct identification of pop-in events in the load–displacement curve not only is dependent on the type of indenters used, but also even very much dependent on the test system and the maximum applied load used. For instance, Kucheyev *et al* [20] reported that the critical load for pop-in to occur varied in the range of ~24–40 mN for GaN films at an indentation load of 100 mN by using ANU UMIS-2000 Nanoindenter Systems with a spherical indenter tip. While, in our previous study [13], we found that the critical load for pop-in actually occurred in the range of ~1.2–1.5 mN for GaN films at an indentation load of 3 mN by using Hysitron Triboscope Nanoindenter Systems with a Berkovich indenter tip. On the other hand, Ma *et al* [21] reported that, although pop-ins were evidently observed with 100 mN load in their system, there were no apparent features of pop-ins in the load–displacement curve when an indentation load of 500 mN was applied. They attributed it to the lack of enough resolution when larger load was applied. Another important feature to be noted is that there is no apparent 'irregularity' on any of the unloading segments, which has been regarded as a signature of absence of phase transformation [4, 18]. The present results are largely in agreement with previous studies on GaN thin films [4, 18, 22], except that the values of the mechanical parameters are different (table 1). We suspect that these discrepancies are mainly due to the various indentation methods used. For instance, the tip–surface contact configuration and stress distribution for the Berkovich indenter tip can be drastically different from that for the spherical tip or Vickers-type indenters.

The physical mechanism of the pop-ins appearing in the load–displacement curve has been extensively discussed in the literature. Among all, crack formation, sudden occurrence of pressure-induced phase transformation, and generation of slip bands due to dislocation propagation during the indentation process were identified to have occurred in different systems. Bradby *et al* [4], using the spherical indenter with a tip radius of 4.2 μm, first observed that in Wurtzite structure GaN films there existed multiple discontinuities upon loading. Since there was no crack and no pressure-induced phase transformation observed in their XTEM investigation, they attributed the main deformation mechanism to nucleation of slip bands on the basal planes. In their more recent studies [22], cracks were found at the intersections of converging $\{1\,1\,1\}$ slip bands in cubic structure GaAs. On the other hand, for hexagonal GaN and ZnO with two slip systems (both the basal and pyramidal planes), although dislocations slipping on one system are impeded by the other during plastic deformation, there were no cracks formed for loads up to as high as 900 mN and 200 mN for GaN and ZnO, respectively [22]. Instead, there was a profound pile-up of the material far from the indenter contact diameter observed, suggesting that dislocations were being punched out into the surrounding material when loading continued. It is interesting to note that the similar multiple pop-ins characteristics were also observed in hexagonal structure InSe and GaSe single crystals [23]. In their high-temperature (370 °C) Vickers diamond indentation experiments performed on $(0\,0\,0\,1)$ N-polar GaN single crystals, Weyher *et al* [24] reported evidence of pressure-induced transition from the wurtzite to the energetically most favourable rocksalt structure a very high load of 2 N. Unfortunately, since there was no load–displacement measurement, it is not clear how the pop-in events correlate with phase transitions. Nevertheless, the above discussions do suggest that multiple pop-ins indeed are specific features of materials with hexagonal lattice structure and geometry of the indenter tip may play an important role in determining the nanoindentation-induced mechanical responses. Thus, in order to identify the deformation mechanisms specific to the Berkovich nanoindentation direct microstructure characterization in the vicinity of the indented area is needed.

The scanning electron microscopy (SEM) observation shown in the inset of figure 1 does not reveal any evidence of material pile-ups and signs of crack formation on the film surface around the indented area. There are no 'pop-outs' on the unloading curves either (figure 1), suggesting that phase

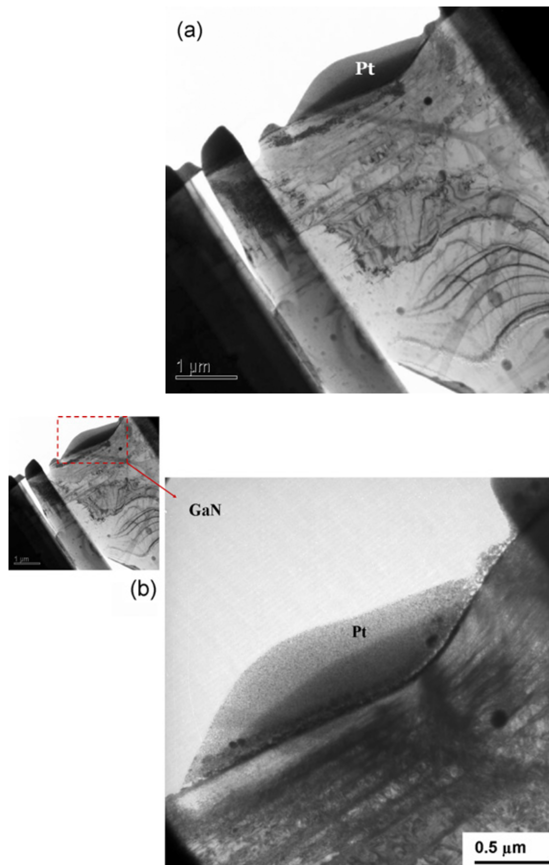

Figure 3. XTEM Bright-field images of specimen after an indentation load to 200 mN. (*a*) A lower magnification photograph showing the regions beneath the indent and part of the substrate. Note that the basal plane slip bands propagate all the way to the film–substrate interface and the stress field appears to extend into the substrate. (*b*) Photograph shows the tangling interactions between dislocations gliding on the two slip systems within a shallower region near the contact surface.

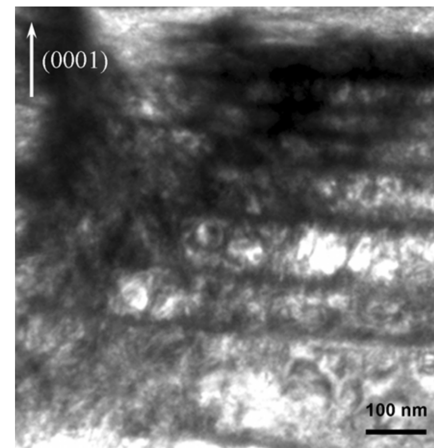

Figure 4. A close-up view of XTEM bright-field image of the heavily deformed region of the GaN thin film, showing that despite of being deformed heavily there is no evidence of crack formation.

transitions like that observed in indented Si [25] are probably not occurring beneath the indenter tip for GaN films. The absence of pop-out serration in the unloading segments load–displacement curves, surface pile-ups, and cracks indicates that nanoindentation-induced deformation in GaN films is predominated by dislocation nucleation and propagations. Figure 3(*a*) shows the bright-field XTEM image, obtained by following the sample preparation procedures illustrated in figure 2, for a GaN film indented with a maximum load of 200 mN by a Berkovich indenter. It is evident from figure 3(*a*) that, for an estimated film thickness of 2 μm, the GaN film studied here shows almost perfect interface epitaxial relations with the sapphire substrate. Moreover, the image clearly displays that, within the film, the deformation features underneath the indented spot are primarily manifested by dislocation activities. Namely the slip bands are well aligned in parallel with the $\{0001\}$ basal planes all the way down to the film–substrate interface. It is also interesting to note that the heavily strained features in the vicinity of the interface may not be just accidental artefacts resulting from sample preparation. They might be direct evidence for displaying that, due to the excellent interface epitaxy between film and substrate, the effects of indentation have, in fact, extended into the sapphire substrate. This argument may also partially explain that, due to the ease of relaxing the local stress right under the indenter's tip via the massive substrate, indentation-induced phase transitions were rarely observed.

In order to have a closer look at the dislocation activities immediately beneath the tip, figure 3(*b*) shows an enlarged XTEM picture in the vicinity of the tip contact region. The picture clearly displays a typical microstructure of a heavily deformed material, characterized by features of very high density of dislocations. Nevertheless, the slip bands (dark thick lines in the photograph) clearly indicate that during the indentation the rapidly increasing dislocations can glide collectively along the easy directions. In the present case, in addition to those aligning parallel to the GaN–sapphire interface along the (0001) basal planes, slip bands oriented at $\sim 60^\circ$ to the sample surface can also be found. The 60° slip bands, which are believed to originate from dislocations gliding along the $\{10\bar{1}1\}$ pyramidal planes, however, are distributed in much shallower regions near the contacting surface. It is indicative that a much higher stress level is needed to activate this slip system as compared with the one along the basal planes. Figure 4 shows a more detailed microstructure near the intersections of the two sets of slip bands. The distorted slip bands and the extremely high dislocation densities at the intersections indicate the highly strained state of the material. However, even at the submicron scale, no evidence of subsurface cracking and film fragmentation was observed. In addition, the selected area diffraction (not shown here) of the heavily damaged regions did not show evidence of newly formed phases either.

From the above observations and discussion, it is apparent that, in the Berkovich indentation scheme, the primary deformation mechanism for GaN films is dislocation nucleation and propagation along easy slip systems, similar to that concluded with a spherical indenter [4]. Since the pop-in events are usually observed after permanent plastic deformation has occurred (50 mN in the present case) and two of the possible mechanisms, the deformation-induced phase transition and fracture of film [26] were basically ruled out, the most likely mechanism responsible for the pop-ins appears to be associated with the activation of dislocation sources [27].

In this scenario, plastic deformation prior to the pop-in event is associated with the individual movement of a small number of newly nucleated and pre-existing dislocations. As the number of dislocations is increased and entangled with each other, large shear stress is quickly accumulated underneath the indenter tip. When the local stress underneath the tip reaches some threshold level, a burst of collective dislocation movement on the easy slip systems is activated, leading to a large release of local stress and a pop-in event on the load–displacement curve. Each of these collective dislocation movements is reflected as a slip band in the indented microstructure displayed in figure 3. Notice that, although the slip bands appeared to stop near the film–substrate interface (figure 3(*a*)), the released stress due to this effect could extend deep into the substrate as mentioned above. Moreover, the narrow spacing of the dense bands of defects and/or dislocations along the basal planes near the surface suggests that, in the later stage of indentation, a large indentation load, such as the 200 mN used in the present experiments, starts to activate extensive slip bands along the 60° pyramidal planes. The extensive interactions between the dislocations slipping along the two slip systems, thus, confined the slip bands in a shallow regime, which, in turn, resulted in a heavily deformed and strain-hardened lattice structure. Finally, we note that the so-called 'slip-stick' behaviour [4], characterized by material pile-ups caused by interactions between the as-grown defects and the indentation-induced dislocations, is not significant in this study. Whether it is due to the insignificant grown-in defect density of our GaN films or to the specific geometric shape of the indenter tip used is not clear at present and further studies may be required to clarify this issue.

4. Conclusion

In summary, a combination of nanoindentation, FIB and TEM techniques has been carried out to investigate the contact-induced structural deformation behaviour in the GaN thin films. The pop-in behaviours displayed in the loading segments of the load–displacement curves performed with a Berkovich diamond indenter tip were explained by the observed microstructure features obtained from XTEM analyses. The results revealed that the primary nanoindentation-induced deformation mechanism in GaN thin films is nucleation and propagation of dislocations, rather than otherwise proposed stress-induced phase transformation or crack formations. It is noted that both the basal and the pyramidal planes of the GaN lattice are acting as the primary slip systems for collective dislocation motions, with the latter being activated at a higher stress state and hence later stage of indentation.

Acknowledgment

This work was partially supported by the National Science Council of Taiwan, under Grants No NSC 96-2112-M-009-017.

References

[1] Morkoc H and Mohammad S N 1995 *Science* **267** 51
[2] Fasol G 1996 *Science* **272** 1751
[3] Cheng G S, Kolmakov A, Zhang Y X, Moskovits M, Munden R, Reed M A, Wang G M, Moses D and Zhang J P 2003 *Appl. Phys. Lett.* **83** 1578
[4] Bradby J E, Kucheyev S O, Williams J S, Wong-Leung J, Swain M V, Munroe P, Li G and Phillips M R 2002 *Appl. Phys. Lett.* **80** 383
[5] Puech P, Demangeot F, Frandon J, Pinquier C, Kuball M, Domnich V and Gogotsi Y 2004 *J. Appl. Phys.* **96** 2853
[6] Bourhis E Le and Patriarche G 2004 *Phil. Mag. Lett.* **84** 373
[7] Li J, Van Vliet K J, Zhu T, Yip S and Suresh S 2002 *Nature* **418** 307
[8] Kim D E and Oh S I 2006 *Nanotechnology* **17** 2259
[9] Jian S R, Fang T H, Chuu D S and Ji L W 2006 *Appl. Surf. Sci.* **253** 833
[10] Li X D, Zhang L and Gao H 2004 *J. Phys. D: Appl. Phys.* **37** 753
[11] Campo M, Ureña A and Rams J 2005 *Scr. Mater.* **52** 977
[12] Jian S R, Fang T H and Chuu D S 2006 *Appl. Surf. Sci.* **252** 3033
[13] Jian S R, Fang T H and Chuu D S 2003 *J. Electron. Mater.* **32** 496
[14] Li X D and Bhushan B 2002 *Mater. Charact.* **48** 11
[15] Oliver W C and Pharr G M 1992 *J. Mater. Res.* **7** 1564
[16] Drory M D, Ager III J W, Suski T, Grzegory I and Porowski S 1996 *Appl. Phys. Lett.* **69** 4044
[17] Nowak R, Pessa M, Suganuma M, Leszczynski M, Grzegory I, Porowski S and Yoshida F 1999 *Appl. Phys. Lett.* **75** 2070
[18] Kucheyev S O, Bradby J E, Williams J S, Jagadish C, Swain M V and Li G 2001 *Appl. Phys. Lett.* **78** 156
[19] Kavouras P, Komninou Ph and Karakostas Th 2007 *Thin Solid Films* **515** 3011
[20] Kucheyev S O, Bradby J E, Williams J S, Jagadish C, Toth M, Phillips M R and Swain M V 2002 *Appl. Phys. Lett.* **77** 3373
[21] Ma L W, Cairney J M Hoffman M J and Munroe P R 2004 *Appl. Surf. Sci.* **237** 631
[22] Bradby J E, Williams J S and Swain M V 2004 *J. Mater. Res.* **19** 380
[23] Mosca D H, Mattoso N, Lepienski C M, Veiga W, Mazzaro I, Etgens V H and Eddrief M 2002 *J. Appl. Phys.* **91** 140
[24] Weyher J L, Albrecht M, Wosinski T, Nowak G, Strunk H P and Porowski S 2001 *Mater. Sci. Eng.* B **80** 318
[25] Bradby J E, Williams J S, Wong-Leung J, Swain M V and Munroe P 2000 *Appl. Phys. Lett.* **77** 3749
[26] Bull S J 2005 *J. Phys. D: Appl. Phys.* **38** R393
[27] Gaillard Y, Tromas C and Woirgard J 2003 *Phil. Mag. Lett.* **83** 553